DOI: 10.71762/0zkg-qn68
Research Paper

Investigation of the Effect of a Nonlinear Ion Concentration Function on the Electromechanical Behavior of Ionic Polymer–Metal Composites

Reza Poureini[1], Hamid Soleimanimehr[2*], Navid Seyedkazem Viliani[3], Ali Abdollahi[2]
[1]Ph.D. Student, Department of Mechanical and Aerospace Engineering, SR.C., Islamic Azad University, Tehran, Iran
[2]Associate Professor, Modern Automotive Research Center, Department of Mechanical and Aerospace Engineering, SR.C., Islamic Azad University, Tehran, Iran
[3]Assistant Professor, Department of Mechanical Engineering, Ab.C., Islamic Azad University, Abhar, Iran
[*]Email of the Corresponding Author: Ha.Sol@iau.ac.ir
Received: July 11, 2025; Revised: August 27, 2025; Accepted: August 30, 2025

Abstract
The effect of nonlinear ion concentration distribution and electric potential gradient on the induced biaxial moments in ionic polymer–metal composite (IPMC) actuators is investigated. To accurately model the bending behavior, a combined approach is employed, integrating the Euler–Bernoulli beam theory, the principle of minimum potential energy, and a nonlinear field- and time-dependent mechanical property model. In this framework, the ion concentration distribution is assumed to be nonlinear along both longitudinal and transverse directions. The coupled electro-ionic interactions are analyzed using the Nernst–Planck and Poisson equations. Numerical results demonstrate that adopting a nonlinear ion distribution leads to nearly equal induced electrical moments in both directions at the mid-plane, significantly reducing biaxial bending and yielding a more balanced deformation profile. This approach yields a 95% reduction in transverse moment compared to the linear model, underscoring the superior effectiveness of the proposed nonlinear method in mitigating undesirable biaxial bending in IPMC actuators.

Keywords
IPMC, Nonlinear Ion Concentration, Euler-Bernoulli Beam, Energy Method, Nernst-Planck, Poisson Equation, Biaxial Bending

1. Introduction
Ionic–metal polymer composites (IPMCs) have garnered significant attention in fields such as soft robotics, biomedical applications, and microelectromechanical systems (MEMS) due to their high flexibility, low-voltage actuation, and ability to operate at small scales [1, 2]. The precise design of multi-material structures can significantly enhance the mechanical properties of polymer composites [3]. An approach that has also been considered for improving the electromechanical performance of IPMC. One of the key challenges in developing smart composites is accurately modeling their mechanical and electromechanical behavior. In particular, at micro- and nanoscale dimensions,

classical models fail to provide precise predictions. Therefore, the Timoshenko beam theory has been extended by incorporating small-scale effects to analyze the bending and vibrational behavior of nanoscale beams more accurately. It has been demonstrated that neglecting these effects yields inaccurate results in modeling micro- and nanoscale structures [4].

By analyzing the Nernst–Planck equation for ionic–metal polymer beams under clamped boundary conditions, it has been found that the maximum stress and displacement are concentrated at the center of the beam and in the electrode regions. This condition is a key insight for designing MEMS and precision actuators [5]. A model based on ion transport has also been developed, which accurately simulates the relationship between input voltage and deformation in IPMCs. The analytical results of this model have shown high accuracy compared to classical models (especially in the case of small deformations) when validated against experimental data [6]. Bending models using resistive electrodes have enabled investigation of the role of electrical conductivity in dynamic responses and voltage distribution [7].

The effect of ionic liquids on the bending behavior of IPMCs has been recently examined. It was found that ions play a significant role in actuation and bending performance and must be considered in precise design [8]. In this regard, the use of hybrid electrodes has enabled the achievement of desired bending deformation and strain under specific voltages, opening a new pathway for the design of assistive devices and human–machine interfaces [9].

Coupled electrochemical–mechanical numerical models have been developed to predict the precise relationship between applied voltage and bending in IPMCs [10]. To enhance durability and conductivity, the use of SWCNT $^{\text{and PEDOT: PSS}}$ electrodes has been proposed, yielding positive results [11].

The bending behavior of copper-based IPMCs has also been investigated, revealing a direct correlation between applied voltage and deformation. For instance, a maximum displacement of 0.42 mm was reported under 5 volts. Moreover, the von Mises stress in the electrodes increases with increasing voltage [12]. Another study examined the effect of time on the bending response of IPMCs with silver electrodes. The results indicate that high voltage causes a faster decay of bending response over time—an exploitable feature in robotics and MEMS applications [13].

Although numerous studies have analyzed and modeled the bending response of IPMCs, most are based on uniaxial bending, evaluating structural response in only one bending direction (typically along the longitudinal axis). However, due to the anisotropic nature and non-uniform distribution of electric and ionic fields in these materials, biaxial bending also occurs. Neglecting this characteristic may lead to significant errors in predicting actual responses and designing accurate functionality. Therefore, the development of models that account for biaxial bending is considered a fundamental research need in the field of IPMCs.

In most previous analyses, including those based on the classical Maxwell approach [14], the focus has been on calculating stresses and electromechanical forces via body or surface force densities. However, these methods, particularly in multiphase and heterogeneous systems like IPMCs—where ionic fields, viscosity, and complex deformations are simultaneously involved—are unable to predict the distribution of moments and biaxial curvature accurately. In this article, an energy-based approach is employed, wherein the bending moments induced by electric fields are directly derived from the system's free energy derivatives. This approach enables precise consideration of the interaction between ion distribution, potential fields, and mechanical response. Unlike the Maxwell model, it does not require explicit calculation of surface forces. As a result, the energy-based method is not only more accurate but also mathematically more consistent, with the capacity to be extended to more complex conditions such as biaxial bending.

Complex mechanical behaviors such as biaxial bending, especially under electrical stimulation, make the precise control of these actuators challenging. These phenomena mainly arise from the interaction between the electric field and the ion distribution. Relying on the Euler–Bernoulli beam theory and the energy method, this paper employs the Nernst–Planck equation to model ion transport and investigate its effect on the electromechanical bending behavior of ionic polymer–metal composites (IPMCs). The governing equations are derived to provide a strategy for reducing biaxial bending by considering the time- and field-dependent nature of mechanical properties such as Young's modulus and shear modulus. The core innovation lies in the formulation of a strain energy model for IPMC actuators, in which the dependencies of both Young's and shear moduli on time and electric field intensity are simultaneously incorporated as combined exponential functions. Moreover, by integrating the Nernst–Planck and Poisson equations with piezoelectric relations, a comprehensive analytical framework is presented to link electrical excitation, ion distribution, and mechanical response. This model enables the analysis of undesired biaxial bending behavior and proposes methods to mitigate it. These innovations represent a significant step forward compared to previous works such as [6-14], which have only addressed uniaxial bending.

2. IPMC Analysis

In the Euler–Bernoulli beam theory, the rotation of cross-sections is considered negligible compared to the displacement. Also, the angular deformation due to shear is neglected in comparison with the bending deformation.

The Euler–Bernoulli beam theory applies to beams whose lengths are significantly greater than their depths (at least 10 times), and whose displacements are small relative to the depth.

It is important to note that the Euler-Bernoulli beam theory assumes small deformations and neglects shear effects. While this provides a simplified analytical framework suitable for many actuator designs, it may not fully capture the behavior of IPMCs under large deformations or with high flexibility. In future studies, the model can be extended using Timoshenko beam theory or nonlinear strain formulations to predict behavior in such scenarios better.

When the transverse displacement of the beam's centerline is denoted by w, the displacement components of any point in the cross-section, assuming that cross-sections remain flat and perpendicular to the centerline, are given as follows [15]:

$$\begin{aligned} u &= -z\frac{\partial w(x,t)}{\partial x} \\ v &= 0 \\ w &= w(x,t) \end{aligned} \tag{1}$$

Where, u, v, and w are the displacement components in the x, y, and z directions, respectively. The corresponding strain and stress components based on this displacement field are given by [15]:

$$\varepsilon_{xx} = \frac{\partial u}{\partial x} = -z\frac{d^2w}{dx^2}$$
$$\varepsilon_{yy} = \varepsilon_{zz} = \varepsilon_{xy} = \varepsilon_{yz} = \varepsilon_{zx} = 0 \tag{2}$$

Here, $w(x)$ is the vertical displacement of the beam. Assuming a linear stress–strain relationship and using Young's modulus E, the stress is given by:

$$\sigma_{xx} = E \cdot \varepsilon = -Ez\frac{d^2w}{dx^2}$$
$$\sigma_{yy} = \sigma_{zz} = \sigma_{xy} = \sigma_{yz} = \sigma_{zx} = 0 \tag{3}$$

The strain energy π of the system can be expressed as follows [15]:

$$\pi = \frac{1}{2}\iiint_V \left(\sigma_{xx}\varepsilon_{xx} + \sigma_{yy}\varepsilon_{yy} + \sigma_{zz}\varepsilon_{zz} + \sigma_{xy}\varepsilon_{xy} + \sigma_{yz}\varepsilon_{yz} + \sigma_{zx}\varepsilon_{zx}\right) = \frac{1}{2}\int_0^l EI\left(\frac{d^2w}{dx^2}\right)^2 dx \tag{4}$$

Where I is the second moment of area of the beam cross-section with respect to the y-axis [15]:

$$I = I_y = \iint_A z^2 dA \tag{5}$$

These relations form the foundation of the classical equilibrium equation for Euler–Bernoulli beams and serve as a starting point for analyzing biaxial bending in IPMCs. For a more accurate assessment of the mechanical behavior of the beam, calculating the bending strain energy based on stress and strain according to the Euler–Bernoulli theory is essential.

In the analysis of ionic–metallic polymer actuators, when the material is subjected to bending in two orthogonal planes (typically the xz and yz planes), the bending strain energy must include both bending components. In this case, the bending curvature along the x-axis is characterized by the vertical displacement $w(x)$, and the transverse bending is described by the lateral displacement $v(y)$. Specifically, the following two curvatures are defined [16]:

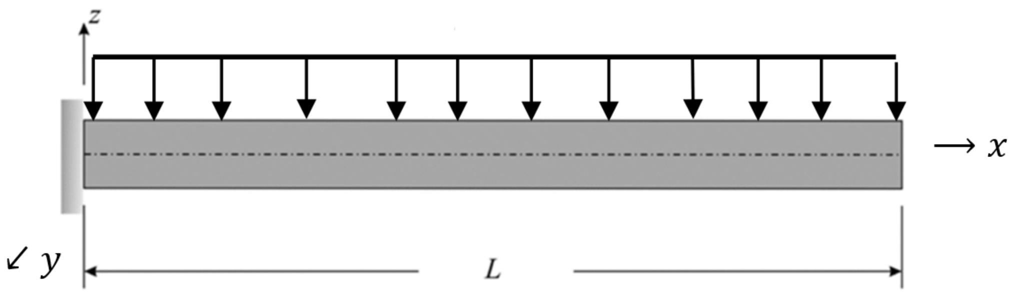

Figure 1. Force induced by applied voltage

Bending of the beam in the xz plane, which represents the longitudinal curvature of the structure, is described by the curvature component. $\kappa_x = \frac{d^2w}{dx^2}$. In this relation, w denotes the vertical displacement along the x-direction. The resistance of this bending against deformation is specified by the bending stiffness EI_x, where E is the Young's modulus of the material and I_x is the second moment of area about the horizontal axis.

On the other hand, bending in the yz plane is referred to as transverse bending, and its corresponding curvature is defined by $\kappa_y = \frac{d^2v}{dy^2}$ Where v represents the displacement in the transverse y direction. The stiffness of this bending is expressed as EI_y, where I_y is the second moment of area with respect to the vertical axis.

Given that the beam has a length-to-width ratio of 10 (Figure 1), and for improved accuracy, the lateral displacement function v is considered as a function of y, and second derivatives with respect to yy are taken into account.

Taking into consideration the contribution of both curvature components in the strain energy, the general form of the total bending strain energy under biaxial bending is expressed as:

$$U_{biaxial-bend} = \frac{1}{2}\int_{-\frac{b}{2}}^{\frac{b}{2}}\int_0^L \left[EI_x\left(\frac{d^2w}{dx^2}\right)^2 + EI_y\left(\frac{d^2v}{dy^2}\right)^2\right]dxdy \tag{6}$$

This equation forms the basis for energy analysis when the material is subjected to loads causing simultaneous bending in two principal directions.

In the Euler–Bernoulli beam theory, the strain energy due to internal bending is given by [15]:

$$U_{bend} = \frac{1}{2}\int_0^l EI\left(\frac{d^2w}{dx^2}\right)^2 dx \tag{7}$$

Now, assume that an external distributed moment is applied along the beam length as a function of x, denoted by $M_{elec}(x)$ (Figure 2). This moment tends to change the curvature of the beam.

The virtual work done by this moment due to the bending of the beam is:

$$\delta w_{elec} = \int_0^l M_{elec}(x) \cdot \delta\left(\frac{d^2 w}{dx^2}\right) dx \tag{8}$$

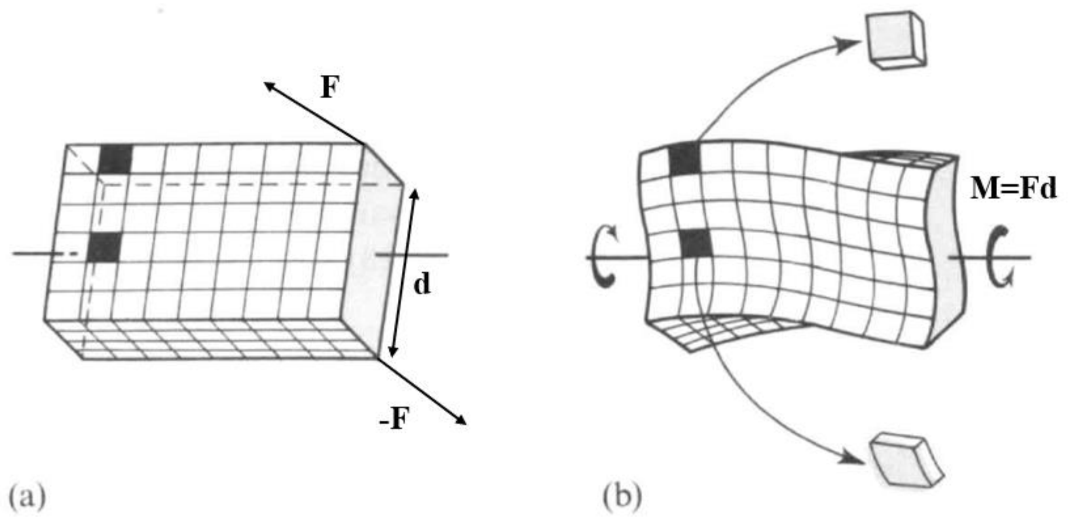

Figure 2. Rectangular shaft (a) before and (b) after applying torque [19]

If we now wish to write the equivalent potential energy of this bending load, by definition:

$$U_{elec} = -w_{elec} = \int_0^L M_{elec}(x) \cdot \frac{d^2 w}{dx^2} dx \tag{9}$$

The negative sign indicates that this energy corresponds to an external force, which appears with a negative sign in the Lagrangian formulation (as opposed to the strain energy, which is positive).
As a result of electrical stimulation, the internal moment arising from ion displacement and the resulting potential gradient in the IPMC is modeled as an external moment in the analysis. The equivalent strain energy due to this moment is modeled as:

$$U_{elec} = -\int_0^L M_{elec}(x) \cdot \frac{d^2 w}{dx^2} dx \tag{10}$$

Where, $M_{elec}(x)$ is the induced electric moment along the beam due to ionic actuation. For the case in which the beam undergoes biaxial bending (i.e., bending occurs both in the xz-plane and in the yz-plane), the electric moments can act in both planes. In this case, the potential energy resulting from the electric moments is expanded as follows:

$$U_{elec} = -\int_0^L \int_{-\frac{b}{2}}^{\frac{b}{2}} \left[M_{elec}^{(w)}(x) \cdot \frac{d^2 w}{dx^2} + M_{elec}^{(v)}(y) \cdot \frac{d^2 v}{dy^2}\right] dxdy \tag{11}$$

As a result, the total potential energy of the system, which is a combination of the biaxial bending energy and the energy resulting from electric actuation, is expressed as follows:

$$\pi = U_{biaxial-bend} + U_{elec}$$

$$\pi = \frac{1}{2}\int_{-\frac{b}{2}}^{\frac{b}{2}}\int_{0}^{L}\left[EI_x\left(\frac{d^2w}{dx^2}\right)^2 + EI_y\left(\frac{d^2v}{dy^2}\right)^2\right]dxdy - \int_{0}^{L}\int_{-\frac{b}{2}}^{\frac{b}{2}}\left[M_{elec}^{(w)}(x)\cdot\frac{d^2w}{dx^2} + M_{elec}^{(v)}(y)\cdot\frac{d^2v}{dy^2}\right]dxdy \tag{12}$$

The first term represents the bending strain energy due to curvature in the longitudinal and transverse directions of the beam; the second term is the potential energy induced by electric actuation, which generates internal bending moments.

2.1 Derivation of Equations Based on the Principle of Minimum Potential Energy

Considering bending in both the xz- and yz-planes, as well as the energy due to ionic actuation, the total potential energy of the system is given by: We use the principle of minimum potential energy ($\delta\pi = 0$), where here $w = w(x)$ is the vertical deflection in the x-direction and $v = v(y)$ is the lateral deflection in the y-direction.

$$\delta\pi = \delta(U_{biaxial-bend} + U_{elec}) \tag{13}$$

Bending energy (the part related to $w(x)$):

$$\delta\pi_w = \int_{-\frac{b}{2}}^{\frac{b}{2}}\int_{0}^{l}\left[EI_x\frac{d^2w}{dx^2}\cdot\frac{d^2\delta w}{dx^2} - M_{elec}^{(w)}(x)\frac{d^2\delta w}{dx^2}\right]dxdy \tag{14}$$

We aim to factor out δw, so we perform integration by parts twice with respect to x. For the first integration by parts, we use the following identity [18]:

$$\int f''(x).\delta w''(x)dx = [f''(x).\delta w'(x)]_0^l - \int f'''(x).\delta w'(x)dx \tag{15}$$

And again for $\delta w'(x)$:

$$\int f'''(x).\delta w'(x)dx = -[f'''(x).\delta w(x)]_0^l + \int f''''(x).\delta w(x)dx \tag{16}$$

Therefore, the entire variation expression becomes:

$$\delta\pi_w = \int_{-\frac{b}{2}}^{\frac{b}{2}}\int_{0}^{l}\left[EI_x\frac{d^4w}{dx^4} - \frac{d^2M_{elec}^{(w)}(x)}{dx^2}\right].\delta w dxdy + B.C. \tag{17}$$

Governing differential equation for bending in the x-direction:

$$EI_x \frac{d^4 w}{dx^4} = \frac{d^2 M_{elec}^{(w)}(x)}{dx^2} \tag{18}$$

In the transverse direction of the beam, the displacement function $v(y)$ describes the bending deformation. To accurately model this deformation, the bending equilibrium equation is used. In this regard, the bending stiffness of the structure is denoted by EI_y, where E is Young's modulus and I_y is the second moment of area about the transverse axis of bending. Accordingly, the bending equilibrium relation is expressed as follows:

$$EI_y \frac{d^4 v}{dv^4} = \frac{d^2 M_{elec}^{(w)}(y)}{dy^2} \tag{19}$$

The remaining terms represent the natural boundary conditions:

$$\delta\pi = \left[\left(EI_x \frac{d^2 w}{dx^2} - M_{elec}^{(w)}(x)\right).\delta w' - \left(\frac{d}{dx}\left(EI_x \frac{d^2 w}{dx^2} - M_{elec}^{(w)}(x)\right).\delta w\right)\right]_{x=0}^{x=l} \tag{20}$$

To examine bending equilibrium, the shear force in this direction is obtained by differentiating the effective bending moment with respect to x. In static equilibrium, this shear force must be zero:

$$V(x) = \frac{d}{dx}\left(EI_x \frac{d^2 w}{dx^2} - M_{elec}^{(w)}(x)\right) = 0 \tag{21}$$

Along the longitudinal direction of the beam, the curvature caused by bending is described by the displacement function $w(x)$. The bending moment in this direction consists of two components: one related to the bending stiffness of the structure (EI_x) and the other arising from the effects of the electric field $M_{elec}^{(w)}(x)$. Therefore, the net or effective bending moment is defined as:

$$M(x) = EI_x \frac{d^2 w}{dx^2} - M_{elec}^{(w)}(x) = 0 \tag{22}$$

To satisfy force equilibrium, the derivative of this moment with respect to y must be zero:

$$V(y) = \frac{d}{dy}\left(EI_y \frac{d^2 v}{dy^2} - M_{elec}^{(v)}(y)\right) = 0 \tag{23}$$

Similarly, in the transverse direction of the beam, the bending displacement function is represented by $v(y)$. The bending moment in this direction is also a combination of transverse bending stiffness EI_y and the moment caused by the transverse electric field $M_{elec}^{(v)}(y)$. The net moment along the y-direction is expressed as:

$$M(y) = EI_y \frac{d^2 v}{dy^2} - M_{elec}^{(v)}(y) = 0 \tag{24}$$

2.2. Electrochemical coupling and biaxial bending generation

The deformation behavior in ionic polymer-metal composite (IPMC) materials under an electric field can be described using the Nernst–Planck equation, which governs ion transport [17]:

$$J = -D\left[\nabla C + \frac{zF}{RT} C.\nabla V\right] \tag{25}$$

Where D is the ion diffusion coefficient $\frac{m^2}{s}$, ∇C is the ion concentration gradient, z is the ion charge number (e.g., positive for cations and negative for anions), F is Faraday's constant (96485 $\frac{Coulombs}{mol}$), R is the universal gas constant $8.314 \frac{J}{mol\,°K}$, T is the absolute temperature $°K$, and ∇V is the electric potential gradient.

The non-uniform distribution of ions causes an osmotic pressure difference between the top and bottom layers of the IPMC, producing non-uniform internal stresses. These stresses lead to bending moments. The electromechanically induced stress is a function of ion concentration and electric potential:

$$\sigma = f(c, V) \tag{26}$$

Where, σ bending and torsional stresses, C is the ion concentration, and V is the voltage. At steady state, the relation is:

$$\nabla \cdot J = 0 \tag{27}$$

To connect the potential field to the ion concentration (ion distribution), the Poisson equation is used [17]:

$$\nabla^2 V + \frac{\rho}{\varepsilon} = \frac{zF(c - c_0)}{\varepsilon} \tag{28}$$

Where, ρ is the charge density, V is the electric potential, ε is the permittivity or dielectric constant of the material, and c_0 is the initial concentration.

Ions, when displaced, create electromechanical stress. This stress is equivalent to a bending moment:

$$M_{elec}^{(w)}(x) \propto \int_{-\frac{h}{2}}^{\frac{h}{2}} z.\sigma_{elec}(z) dz \tag{29}$$

Where, σ_{elec} is a function of the distributions of V and c.

Now, to reduce biaxial bending, the voltage application pattern can be modified, or by applying gradient electric field patterns, the moments $M_{elec}^{(w)}$ and $M_{elec}^{(v)}$ can be driven toward equilibrium or one of them can be neutralized.

Specifically, we want the direction of the biaxial bending to satisfy:

$$\kappa_x \approx \kappa_y \quad \Rightarrow \quad M_{elec}^{(w)}(x) \approx M_{elec}^{(v)}(y) \tag{30}$$

3. Fundamental Relations of Piezoelectric Materials

The fundamental properties of a piezoelectric material are expressed as relations between two mechanical variables (stress and strain) and two electrical variables (electric field and electric displacement).

The expressions for the direct and converse piezoelectric effects can be combined into a matrix equation. In this case, the relationship between strain and electric displacement is written as a function of applied stress and electric field [20]:

$$\begin{Bmatrix} S \\ D \end{Bmatrix} = \begin{bmatrix} s & d \\ d & \varepsilon \end{bmatrix} \begin{Bmatrix} T \\ E \end{Bmatrix} \tag{31}$$

Where S is the strain vector, T is the stress vector, D is the electric displacement vector, E is the electric field vector, s is the compliance tensor, ε is the dielectric tensor, and d is the piezoelectric coefficient matrix.

3.1 Influence of Mechanical and Electrical Boundary Conditions

The behavior of piezoelectric materials is significantly affected by electrical and mechanical boundary conditions. Depending on whether electrical variables (electric field or displacement) or mechanical variables (stress or strain) are controlled or held fixed at the boundaries, the material response can vary considerably.

In the first case (short circuit), the electrodes are connected, resulting in an electric field of zero. By setting $E = 0$ in the piezoelectric relations:

$$\begin{aligned} S &= sT \\ D &= dT \end{aligned} \tag{32}$$

In the second case (open circuit), the electric displacement at the boundaries is zero; i.e., no free charge can move. Applying the condition $D = 0$:

$$T = \frac{1}{s(1-k^2)} S \tag{33}$$

$$E = \frac{k^2}{d(1-k^2)} S \tag{34}$$

Where:

$$k^2 = \frac{d^2}{s\varepsilon} \tag{35}$$

is the electromechanical coupling coefficient.

3.2 Modeling with E and G Dependence

In soft polymeric materials, mechanical properties such as Young's modulus and shear modulus are sensitive to external factors; the electric field alters the molecular structure and ion movement, resulting in the material becoming softer or stiffer. Time also affects behavior because these materials are viscoelastic—they exhibit properties between those of solids and liquids and change over time. In many material models (especially polymers), mechanical properties such as E or G may depend on physical fields like the electric field. This dependence is often modeled exponentially because it effectively captures rapid or nonlinear changes and matches experimental results in many materials. Differential equations related to these models are easier to solve.

To consider the variability of E and G in the strain energy analysis of IPMC, the following methods can be used: Make E and G dependent on the electric field.

Since some experimental studies have observed that the mechanical properties of soft polymeric materials, such as Young's modulus and shear modulus, decrease under the influence of an electric field and over time, in this research, for simplicity of analysis and feasibility of modeling dependent phenomena, it has been assumed that this dependency can be defined exponentially as a combination of time and field. The following relations are proposed as a model, with the goal of examining the overall behavior of the system under this simplified assumption, rather than providing an accurate empirical model (equations (36) to (41)). Therefore, these parameters can be modeled as functions of the electric field intensity E_f:

$$E(E_f) = E_0 e^{-\gamma E_f} \tag{36}$$

$$G(E_f) = G_0 e^{-\delta E_f} \tag{37}$$

Where:

e is the base of the natural logarithm, approximately equal to 2.718. This exponential function shows that the shear modulus G decreases exponentially with increasing electric field intensity E_f.

γ and δ are constants that must be determined experimentally.

$E_f = \frac{U}{d}$ is the electric field intensity calculated from the voltage U and thickness d.

These relations indicate that increasing the electric field leads to a decrease in both Young's modulus and shear modulus, which is observed in many soft materials.

Modeling as a Time-Dependent Function

If time dependency is also considered, a viscoelastic model can be used:

$$E(t) = E_0 + E_1 e^{-\frac{t}{\tau}} \tag{38}$$

$$G(t) = G_0 + G_1 e^{-\frac{t}{\tau}} \tag{39}$$

Where:

E_1 and G_1 represent the initial changes in stiffness.

τ is the time constant indicating how the material changes over time.

Combining the electric field dependency and the time dependency methods provides accurate results for modeling the mechanical properties of IPMCs (Ionic Polymer-Metal Composites), because both electrical stimulation effects and viscoelastic behavior influence deformation. Below is an explanation of how these two methods are combined:

Combined Model for Young's Modulus

Considering that both time and electric field affect E, it is defined as:

$$E(t, E_f) = \left(E_0 + E_1 e^{-\frac{t}{\tau}}\right) e^{-\gamma E_f} \quad (40)$$

where:

E_0 is the initial modulus in the dry state.

E_1 indicates the modulus reduction due to viscoelastic properties.

τ is the time constant related to the relaxation process.

γ is an empirical coefficient representing the effect of the electric field.

$E_f = \frac{U}{d}$ is the electric field intensity.

This relation considers two essential points:

Viscoelasticity: $E(t)$ decreases over time.

Electric field effect: Increasing E_f reduces the material stiffness.

1. Combined Model for Shear Modulus

Similarly, G is defined as:

$$G(t, E_f) = \left(G_0 + G_1 e^{-\frac{t}{\tau}}\right) e^{-\delta E_f} \quad (41)$$

where the values G_0, G_1, τ, and δ are analogous to those in the E model.

Shear modulus also decreases over time due to the viscoelastic behavior of the material. Increasing the electric field causes a reduction in shear stiffness, which is crucial for the bending behavior of IPMCs.

To evaluate the accuracy of the presented analytical model, its results were compared with those of the numerical model based on the Nernst-Planck equation and energy analysis. In the numerical model, by applying realistic boundary conditions and utilizing a nonlinear distribution of the electric field, the bending moment distribution in both longitudinal and transverse directions of the beam was determined, and the resulting curvatures in each direction were calculated. Then, using the time-dependent analytical model and the electric field-dependent model for E and G, the strain and curvature under similar conditions were estimated. The convergence of the analytical and numerical results demonstrated that the analytical model accurately describes the bending behavior of IPMC. Additionally, the overall trend of reduced biaxial bending in response to field and time settings was observed similarly in both models, which further confirms the validity of the analytical model.

The exponential dependency of Young's and shear moduli on time and electric field is proposed as a theoretical approach based on observed trends in polymer behavior. The coefficients used in equations (40) and (41) are illustrative and not derived from direct experimental measurements. Future work should focus on calibrating these parameters using empirical data.

4. Numerical Model

The goal is to reduce the difference between $M_{elec}^{(w)}(x)$and $M_{elec}^{(v)}(y)$ to minimize biaxial bending. Problem data:

Table 1. Section names of the structural members assigned in the analysis

Parameter	Value	Unit
Beam length L	0.2	m
Beam width b	0.02	m
Thickness h	0.001	m
Ion diffusion coefficient D	10^{-9}	$\frac{m^2}{s}$
Ion mobility μ	5×10^{-8}	$\frac{m^2}{V.s}$
Dielectric constant ε	6×10^{-10}	$\frac{C^2}{N.m^2}$
Initial ion concentration c_0	1000	$\frac{mol}{m^3}$
Faraday constant F	96485	$\frac{C}{mol}$
Applied voltage V	2	V
Temperature T	300	K

Calculation of the electric field:

$$E_f = \frac{V}{h} = \frac{2}{0.001} = 2000\frac{V}{m} \tag{42}$$

Using the exponential model for E:

$$E(t) = E_0 + E_1 e^{-\frac{t}{\tau}} \quad , \quad M_{elec}^{(w)}(x) \propto \frac{\partial c}{\partial x} \tag{43}$$

Now, we assume a nonlinear distribution solution for the concentration along the x and y directions.

$$c(x) = c_0\left[1 + \alpha\left(\frac{x}{L}\right) + \alpha_2\left(\frac{x}{L}\right)^2\right] \implies \frac{dc}{dx} = c_0\left[\frac{\alpha}{L} + 2\alpha_2\frac{x}{L}\right] \tag{44}$$

Similarly, along y-direction:

$$c(y) = c_0\left[1 + \beta\left(\frac{y}{b}\right) + \beta_2\left(\frac{y}{b}\right)^3\right] \implies \frac{dc}{dy} = c_0\left[\frac{\beta}{b} + 3\beta_2\left(\frac{y}{b}\right)^2 \cdot \frac{1}{b}\right] \tag{45}$$

A second-degree model (x^2) is suitable for symmetric behavior along the beam's length, while a third-degree model (y^3) better captures edge effects across the beam's width.

Electric moments (proportional to ion gradient × thickness):

Longitudinal direction (x):

$$c_0\left[\frac{\alpha}{L}+2\alpha_2\frac{x}{L}\right]\cdot h=\frac{dc}{dx}\cdot h\propto M_{elec}^{(w)}(x) \tag{46}$$

Transverse direction (y):

$$c_0\left[\frac{\beta}{b}+3\beta_2\left(\frac{y}{b}\right)^2\cdot\frac{1}{b}\right]\cdot h=\frac{dc}{dy}\cdot h\propto M_{elec}^{(v)}(y) \tag{47}$$

Now, using equations (44) to (47) as well as the values in Table (1), the electric moments at the specific point $x = L/2$ and $y = b/2$ are calculated using the proposed nonlinear model.

$$\frac{dc}{dx}=c_0\left[\frac{\alpha}{L}+2\alpha_2\frac{x}{L}\right]\Rightarrow\ \frac{dc}{dx}=1500\,\frac{mol}{m}\Rightarrow M_{elec}^{(w)}(x)=h.\frac{dc}{dx}=1.5\,\frac{mol}{m} \tag{48}$$

$$\frac{dc}{dy}=c_0\left[\frac{\beta}{b}+3\beta_2\left(\frac{y}{b}\right)^2\cdot\frac{1}{b}\right]\Rightarrow\frac{dc}{dy}=9375\,\frac{mol}{m}\Rightarrow M_{elec}^{(v)}(y)=\frac{dc}{dy}\cdot h=9.375 \tag{49}$$

Now, using the values obtained from equations (48) and (49), the ratio of the moments is given by equation (50):

$$\frac{M_{elec}^{(v)}(y)}{M_{elec}^{(w)}(x)}=6.25\Rightarrow M_{elec}^{(v)}(y)=6.25M_{elec}^{(w)}(x) \tag{50}$$

This condition means that the transverse moment in the y-direction is approximately 6six times greater than the longitudinal moment, but it has decreased significantly compared to the linear model (by about 30 times). By adjusting the coefficients of the nonlinear model for the distribution of ion concentration in the longitudinal and transverse directions to achieve nearly equal and physically reasonable bending moments, we assume that $\alpha_2 = 0.2, \alpha = 0.1$, and $\beta = 0.3, \beta_2 = -0.096$.

The values of the electric moments at the specific point $x = L/2$ and $y = b/2$ are calculated using the proposed nonlinear model:

$$\begin{aligned}\frac{dc}{dx}=c_0\left[\frac{\alpha}{L}+2\alpha_2\frac{x}{L}\right]=1000\times)0.5+1(=1500\ \rightarrow\ M_{elec}^{(w)}(x)=\frac{dc}{dx}\cdot h\\ =1500\times0.001=1.5\,\frac{mol}{m}\end{aligned} \tag{51}$$

$$\begin{aligned}\frac{dc}{dy}=c_0\left[\frac{\beta}{b}+3\beta_2\left(\frac{y}{b}\right)^2\cdot\frac{1}{b}\right]=1000\times(15-13.5)=1500\ \rightarrow\ M_{elec}^{(v)}(y)=\frac{dc}{dy}\cdot h\\ =1500\times1.5=1.5\,\frac{mol}{m}\end{aligned} \tag{52}$$

That this:

$$M_{elec}^{(v)}(y) = M_{elec}^{(w)}(x) \tag{53}$$

To reduce biaxial bending, using a controlled nonlinear distribution of ionic concentration, the nonlinear coefficients α_2 and β_2 were adjusted such that the electric moments in both directions at the midpoint of the member are equal. This approach reduces unwanted curvature in the transverse direction, thereby improving the targeted performance of the IPMC.

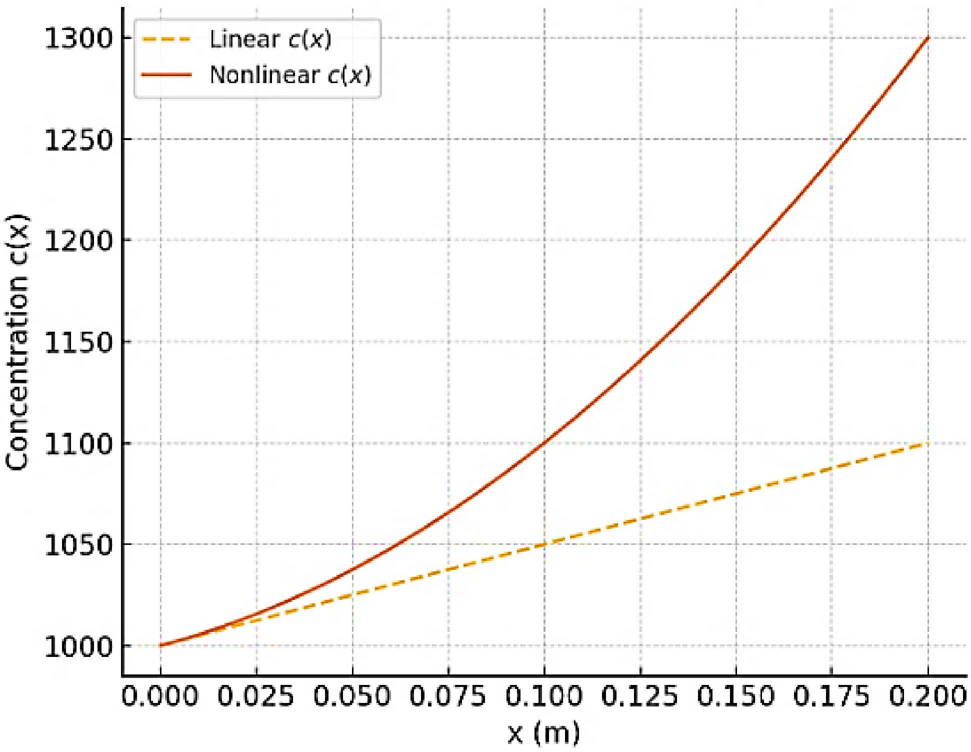

Figure 3. Linear and nonlinear distribution of ions in the longitudinal direction

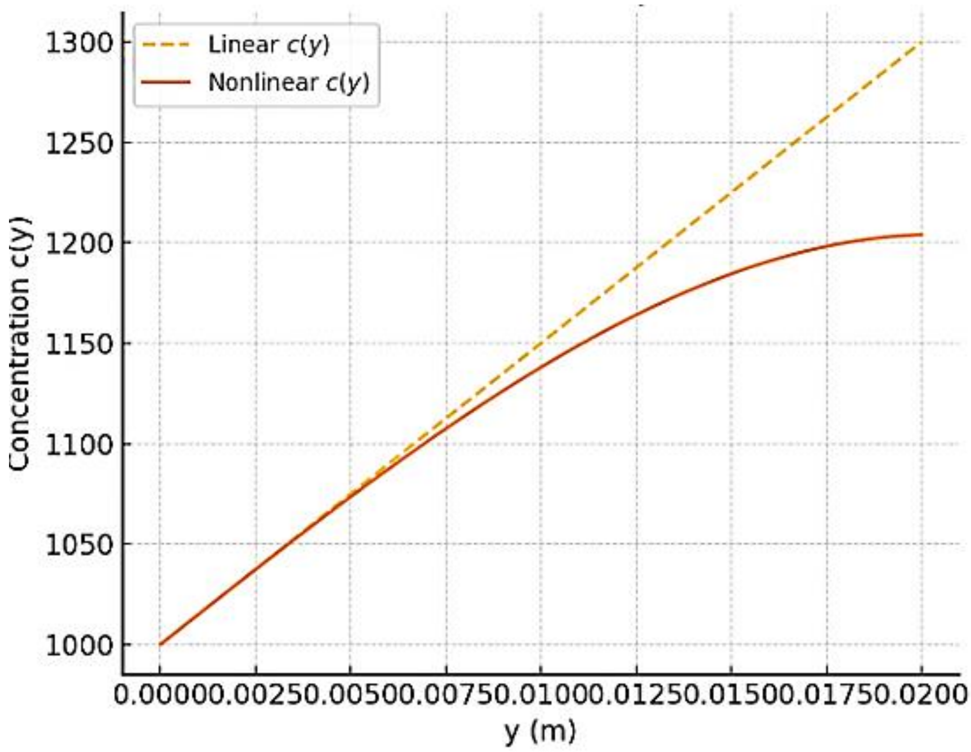

Figure 4. Linear and nonlinear distribution of ions in the transverse direction

In the above diagram, the linear and nonlinear distribution of ions has been compared along the longitudinal direction x and the transverse direction y using equations (44) and (45); these coefficients have been adjusted so that at the central point $x = L/2$ and $y = b/2$, the electric moments in both directions are approximately equal.
Modeling the Young's modulus dependence on the field to neutralize bending effects:

$$E(t, E_f) = \left(E_0 + E_1 e^{-\frac{t}{\tau}}\right) e^{-\gamma E_f} \tag{54}$$

If the goal is to reduce the curvature caused by the electric moment, one must counteract by increasing stiffness (increasing E) in regions with greater curvature; however, by changing the electrodes or modifying the geometry and loading, the effective field magnitude across the width can be reduced (for example, by insulation or spacing). Consequently, bending in the two directions reaches equilibrium, and the biaxial bending decreases.

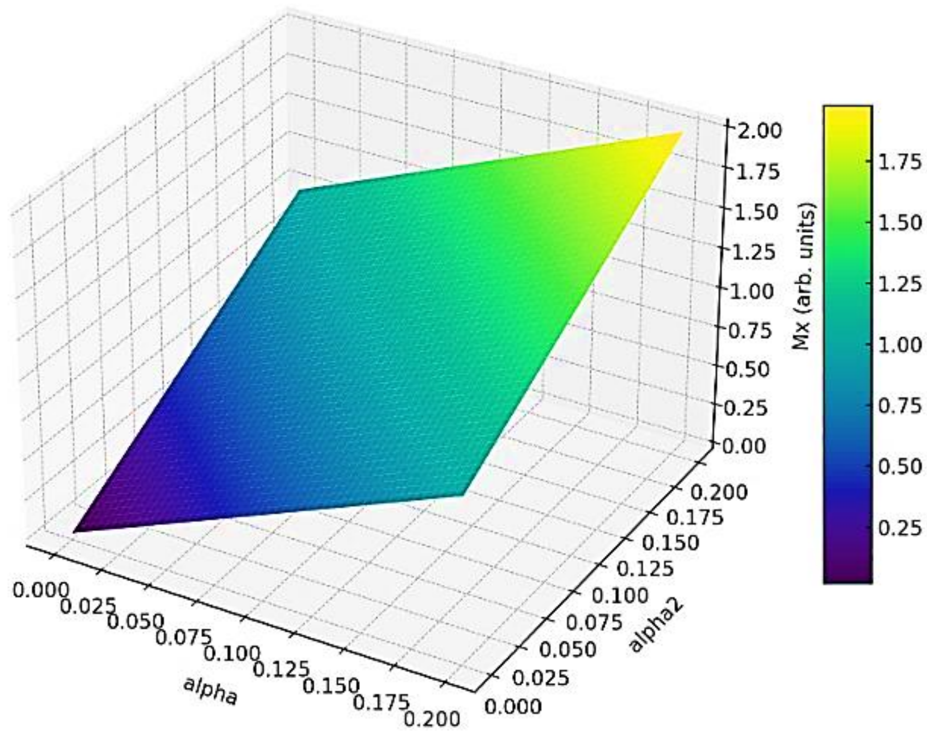

Figure 5. Sensitivity of the longitudinal moment $M_{elec}^{(w)}(x)$with respect to variations in parameters α and α_2

In this three-dimensional plot, the sensitivity of the longitudinal moment $M_{elec}^{(w)}(x)$ to changes in parameters α and α_2 is shown. As is evident, increasing either α or α_2 causes a linear increase in the moment $M_{elec}^{(w)}(x)$.

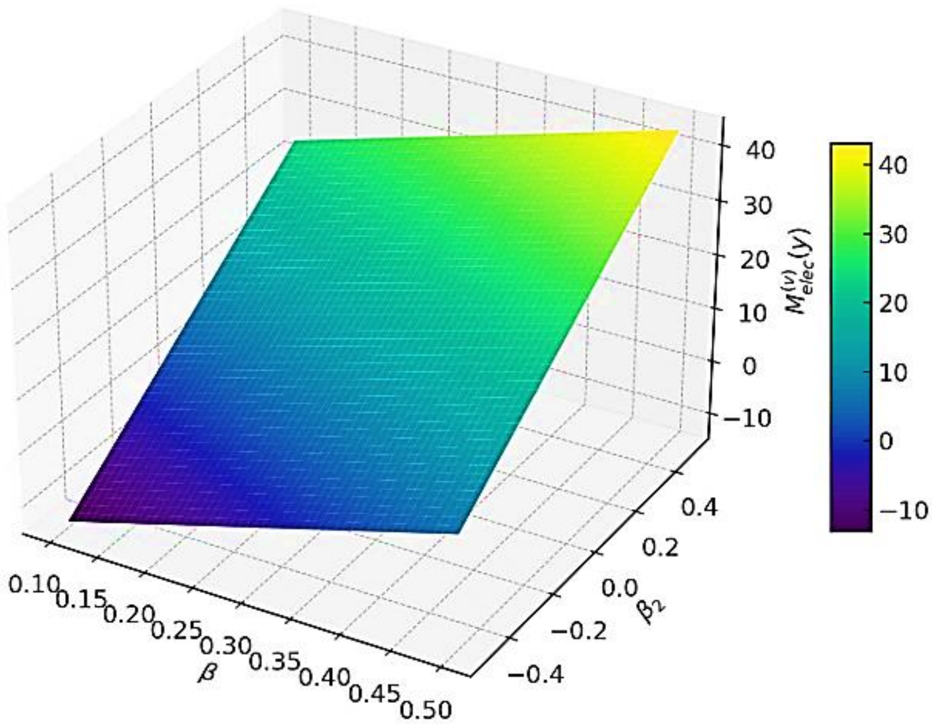

Figure 6. Sensitivity of the transverse moment $M_{elec}^{(v)}(y)$ with respect to variations in the two parameters β and β_2

In this three-dimensional plot, the sensitivity of the transverse moment $M_{elec}^{(v)}(y)$ to changes in the two parameters β and β_2 is illustrated. It is clearly observed that both parameters play a crucial role in shaping the concentration gradient and, consequently, the magnitude of the transverse moment. This analysis aids in the optimal selection of β and β_2 to achieve a balance between longitudinal and transverse moments.

The reduction of the transverse moment was achieved through numerical modeling and by decreasing the effective field intensity across the sample using a hypothetical configuration. In practice, this can be implemented by designing patterned electrodes, insulating certain surface regions, or applying a non-uniform voltage profile. However, such adjustments may lead to a reduction in generated force or an increase in response time, which should be experimentally optimized to achieve the desired outcome.

5. Conclusion

In this paper, a Multiphysics analytical model was developed to more accurately analyze biaxial bending in ionic polymer–metal composite (IPMC) actuators. Unlike classical models, the proposed approach incorporates the time- and field-dependent behavior of Young's modulus and shear modulus to more realistically reflect the material's response under electrical stimulation and over time.

By combining the Euler–Bernoulli beam theory, the principle of minimum potential energy, and the Nernst–Planck and Poisson equations, the interaction between ionic distribution, electric potential gradient, and mechanical response was comprehensively modeled. To further enhance the control of biaxial bending, a nonlinear ion concentration distribution was assumed and analyzed along both longitudinal and transverse directions. This nonlinear profile enabled the independent adjustment of concentration gradients in each direction, leading to more targeted tuning of the induced electrical moments.

Numerical results revealed that an imbalance in ionic concentration gradients along the two principal directions induces unequal electric moments, leading to significant biaxial bending. By refining the potential distribution and precisely controlling the ionic gradients, a better balance between the moments was achieved, and biaxial curvature was significantly reduced. In the linear model, the transverse electric moment was up to 30 times greater than the longitudinal one, causing substantial and undesirable transverse bending. However, by applying the nonlinear distribution, the induced moments reached equilibrium, and the transverse moment was reduced by up to **95%** compared to the linear case. This significant reduction confirms the high effectiveness of the proposed model in mitigating biaxial bending and improving the mechanical performance of IPMCs.

The geometry of the electrode and its surface resistance play a significant role in the distribution of the electric field. In this study, the electric field distribution has been modeled abstractly; however, in future work, electrode heterogeneity can be explicitly incorporated into the model. The use of segmented or resistive electrodes could lead to better control of the biaxial bending.

The presented model not only offers high accuracy in behavior prediction but also provides sufficient flexibility for calibration with experimental data, making it a powerful tool for the targeted design of IPMC actuators in advanced applications, such as micro-robotics, nanotechnology, and biomedical engineering.

6. References

[1] Shahinpoor, M., Bar-Cohen, Y., Simpson, J.O. and Smith, J. 1998. Ionic polymer-metal composites (IPMCs) as biomimetic sensors, actuators and artificial muscles-a review. Smart materials and structures. 7(6):15. doi:10.1088/0964-1726/7/6/001.

[2] López-Díaz, A., Vázquez, A.S. and Vázquez, E. 2024. Hydrogels in soft robotics: Past, present, and future. ACS nano. 18(32):20817-20826. doi:10.1021/acsnano.3c12200.

[3] Salami, S.J., Soleimanimehr, H., Maghsoudpour, A. and Etemadi Haghighi, S. 2023. Fabrication of polycaprolactone/chitosan/hydroxyapatite structure to improve the mechanical behavior of the hydrogel-based scaffolds for bone tissue engineering: Biscaffold approach. Polymer composites. 44(8):4641-4653. Doi:10.1002/pc.27428.

[4] Wang, C.M., Kitipornchai, S., Lim, C.W. and Eisenberger, M. 2008. Beam bending solutions based on nonlocal Timoshenko beam theory. Journal of Engineering Mechanics. 134(6):475-481. doi:10.1061/(ASCE)0733-9399(2008)134:6(475).

[5] Nasrollah, A., Soleimanimehr, H. and Bafandeh Haghighi, Sh. 2024. IPMC-based actuators: An approach for measuring a linear form of its static equation. Heliyon. 10(4):24687. doi:10.1016/j.heliyon.2024.e24687.

[6] Annabestani, M., Naghavi, N. and Maymandi-Nejad, M. 2021. A 3D analytical ion transport model for ionic polymer metal composite actuators in large bending deformations. Scientific reports. 11(1):6435. doi:10.1038/s41598-021-85776-4.

[7] Buchberger, G. and Schoeftner, J. 2013. Modeling of slender laminated piezoelastic beams with resistive electrodes—comparison of analytical results with three-dimensional finite element calculations. Smart materials and structures. 22(3):032001. doi:10.1088/0964-1726/22/3/032001.

[8] Boldini, A. 2024. A multi-cation model for the actuation of ionic membranes with ionic liquids. Materials Advances. doi:10.1039/d4ma00097h.

[9] Saccardo, M.C., Barbosa, R., Zuquello, A.G., Blanco, G.E.D.O., Tozzi, K.A., Gonçalves, R. and Scuracchio, C.H. 2024. Beyond static: Tracking the dynamic nature of water absorption and Young’s modulus in IPMC devices. Journal of Applied Polymer Science. 141(31):55730. doi:10.1002/app.55730.

[10] Soleimanimehr, H. and Bafandeh Haghighi, Sh. Nasrollah, A. 2026. Experimental Analysis of the Effect of Mechanical Topology on the Surface of Biological Microgripper Made of Ionic-Polymer Metal Composite Smart Material. Mechanics of Advanced Composite Structures. doi:10.22075/macs.2024.33962.1670.

[11] Tao, H., Hu, G., Lu, S., Li, B., Zhang, Y. and Ru, J. 2024. Single-Walled Carbon Nanotube-Reinforced PEDOT: PSS Hybrid Electrodes for High-Performance Ionic Electroactive Polymer Actuator. Materials. 17(10):2469. doi:10.3390/ma17102469.

[12] Soleimanimehr, H. and Nasrollah, A. 2021. A numerical investigation the effects of the voltage on the displacement and stress of copper-based ionic polymer-metal composites. Journal of Modern Processes in Manufacturing and Production. 10(1):77-86. dor:20.1001.1.27170314.2021.10.1.6.5.

[13] Biswal, D.K. and Nayak, B. 2016. Analysis of time dependent bending response of Ag-IPMC actuator. Procedia Engineering. 144:600-606. doi:10.1016/j.proeng.2016.05.047.

[14] Boldini, A. and Porfiri, M. 2020. Multiaxial deformations of ionic polymer metal composites. International Journal of Engineering Science. 149:103227. doi:10.1016/j.ijengsci.2020.103227.

[15] Rao, S.S. 2019. Vibration of continuous systems. John Wiley & Sons.

[16] Ugural, A.C. 2009. Stresses in beams, plates, and shells. CRC press. doi:10.1201/b17516.

[17] Shahinpoor, M. ed. 2015. Ionic Polymer Metal Composites (IPMCs): Smart Multi-Functional Materials and Artificial Muscles, Volume 2. Royal Society of Chemistry. doi:10.1039/9781782627234.

[18] Gelfand, I.M. and Silverman, R.A. 2000. Calculus of variations. Courier Corporation.

[19] Mechanics of materials Popov 2th edition Egor P. Popov.

[20] Leo, D.J. 2007. Engineering analysis of smart material systems. John Wiley & Sons. doi:10.1002/9780470209721.